ACS APPLIED MATERIALS & INTERFACES

Research Article

www.acsami.org

Small-Area, Resistive Volatile Organic Compound (VOC) Sensors Using Metal–Polymer Hybrid Film Based on Oxidative Chemical Vapor Deposition (oCVD)

Xiaoxue Wang,[†] Sichao Hou,[‡] Hilal Goktas,[†] Peter Kovacik,[†] Frank Yaul,[§] Arun Paidimarri,[§] Nathan Ickes,[§] Anantha Chandrakasan,[§] and Karen Gleason*[,†]

[†]Department of Chemical Engineering and [§]Department of Electrical Engineering and Computer Science, Massachusetts Institute of Technology, Cambridge, Massachusetts 02139, United States

[‡]Department of Chemical Engineering, Tsinghua University, Beijing 100084, China

Supporting Information

ABSTRACT: We report a novel room temperature methanol sensor comprised of gold nanoparticles covalently attached to the surface of conducting copolymer films. The copolymer films are synthesized by oxidative chemical vapor deposition (oCVD), allowing substrate-independent deposition, good polymer conductivity and stability. Two different oCVD copolymers are examined: poly(3,4-ethylenedioxythiophene-*co*-thiophene-3-aceticacid)[poly(EDOT-*co*-TAA)] and poly-(3,4-ehylenedioxythiophene-*co*-thiophene-3-ethanol)[poly-(EDOT-*co*-3-TE)]. Covalent attachment of gold nanoparticles to the functional groups of the oCVD films results in a hybrid system with efficient sensing response to methanol. The response of the poly(EDOT-*co*-TAA)/Au devices is found to be superior to that of the other copolymer, confirming the importance of the linker molecules (4-aminothiophenol) in the sensing behavior. Selectivity of the sensor to methanol over *n*-pentane, acetone, and toluene is demonstrated. Direct fabrication on a printed circuit board (PCB) is achieved, resulting in an improved electrical contact of the organic resistor to the metal circuitry and thus enhanced sensing properties. The simplicity and low fabrication cost of the resistive element, mild working temperature, together with its compatibility with PCB substrates pave the way for its straightforward integration into electronic devices, such as wireless sensor networks.

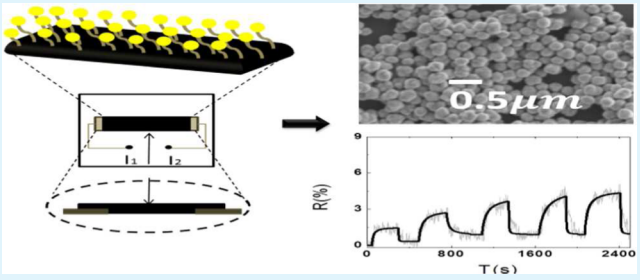

KEYWORDS: *printed circuit board, gold nanoparticle, sensor, oCVD, conducting polymer*

1. INTRODUCTION

Volatile organic compounds (VOCs) raise safety issues in much of the chemical industry.[1] As an important alcohol precursor and the main component in biodiesel production, methanol is among the VOCs that attract the most attention. Therefore, early and reliable detection of methanol is critical to ensure industrial safety. Detection of VOCs using distributed wireless sensor systems has been proposed as an effective tool for monitoring large and complex processing plants.[2] These rely on small and low-cost chemical sensors densely distributed across the facility to form an interconnected low-power wireless network. We demonstrate a novel low-cost methanol sensor based on polymer–nanoparticle films that can be deposited onto printed circuit boards and hence is readily applicable to such sensor network system in refineries.

Sensors based on gold nanoparticles have shown excellent performance in methanol sensing.[3] Previously, researchers have studied chemiresistive devices based on self-assembled films of thiol-functionalized gold nanoparticles.[4] The resistive response derived from film swelling, which impeded electron hopping conduction,[4,5] whereas the selectivity was achieved via the thiol terminal group.[6] Even though functionalized gold nanoparticles can be tailored for many device platforms and act as a good sensing material for a variety of vapors and gases, there are still several device integration issues to be resolved. These issues include difficulty in fabricating reliable electric contacts and poor film durability that limits the lifetime of the sensor. For example, the monolayer Au nanoparticle devices require electrodes fabricated by electron-beam evaporator,[7] and because of lack of covalent bonds between the monolayer and the substrate, the films are subject to delamination and thus device failure.

We demonstrate a novel approach to produce robust sensing elements in a facile and reliable manner. Oxidative chemical vapor deposition (oCVD) technique is a versatile and substrate-independent method for fabrication of well-adhered conducting polymer films which can be used as a platform to anchor the gold nanoparticles and improve the robustness of the sensor. The resistive response of the nanoparticle/polymer films is used to detect the presence of VOCs. The oCVD deposition of

Received: February 3, 2015
Accepted: July 15, 2015
Published: July 15, 2015

DOI: 10.1021/acsami.5b05392
ACS Appl. Mater. Interfaces 2015, 7, 16213–16222

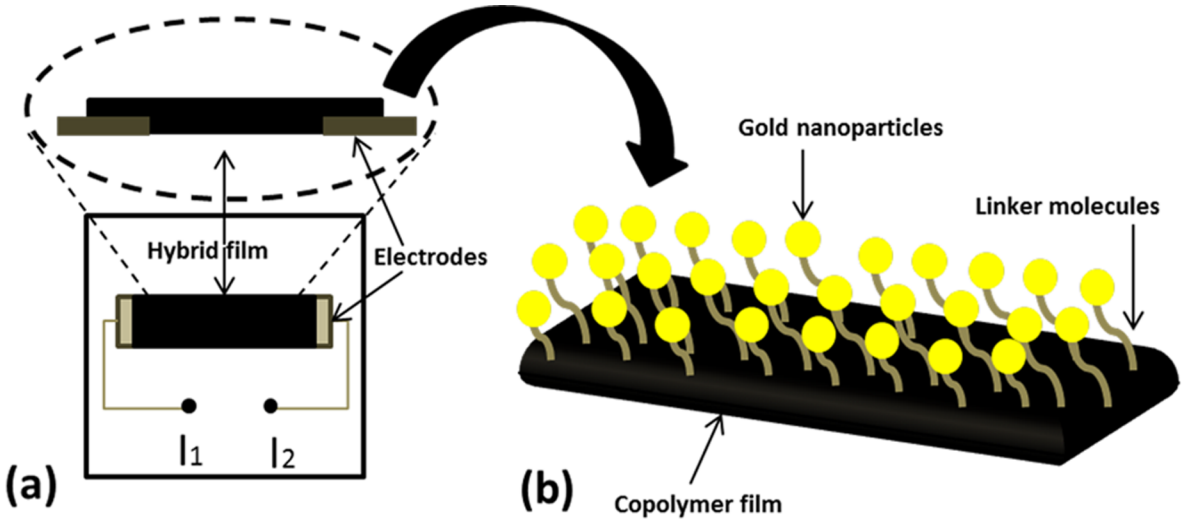

Figure 1. (a) Schematic of the of hybrid films additively patterned as resistive elements directly onto a printed circuit board (PCB). (b) Schematic of the gold nanoparticle/polymer hybrid film. The gold nanoparticles were tethered covalently to the copolymer films by linker molecules.

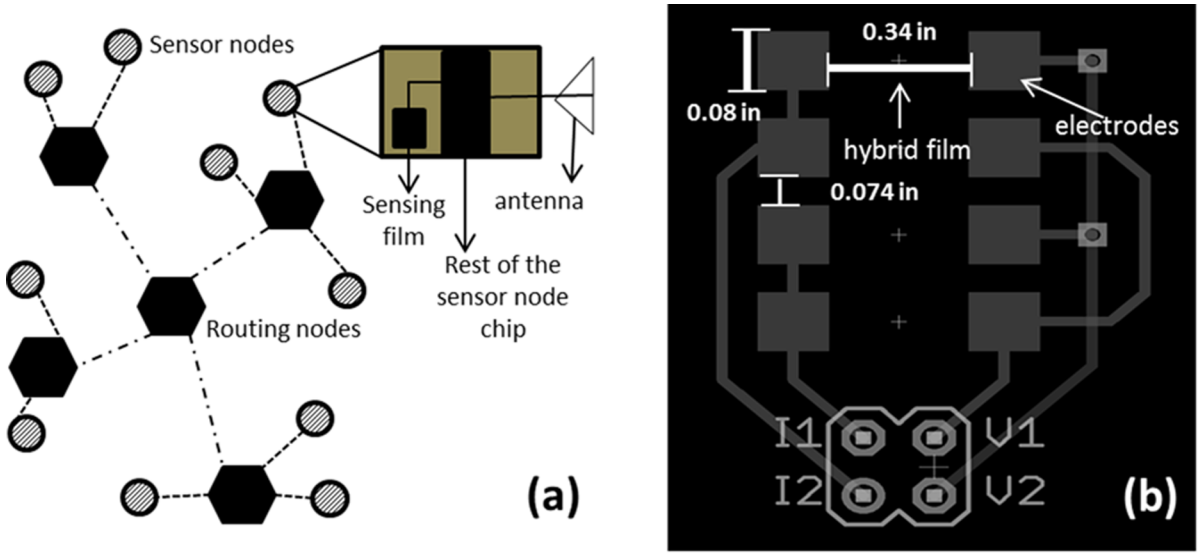

Figure 2. (a) Schematic of a wireless sensor network architecture.[14] The gray circles are sensor nodes, and the black hexagons are routing nodes which coordinate the information from sensors and other routing nodes. The insert is a proposed structure of the sensor node. Our main target is to provide a suitable sensing film in this node. (b) The design of the printed circuit board (PCB) for our sensor.

hybrid films was first described by Vaddiraju et al.[8,9] The metal nanoparticles were grafted onto the surface of the functionalized conducting copolymer films using thiol as the linker molecule.[10,11] The metal nanoparticles remained attached even after 5 min of sonication, demonstrating an excellent durability.[8] The current work builds upon the previous approach by functionalizing gold nanoparticles with new linker chemistry and providing covalent bonding between the conducting copolymers and the gold nanoparticles. Benefiting from the solvent-free character of the oCVD deposition, the hybrid films are additionally patterned directly onto printed circuit boards (PCBs) to prove suitability of the technology for integration into wireless circuits. The architecture of the sensor is shown in Figure 1a and the structure of the hybrid film is depicted in Figure 1b.

We demonstrate high sensitivity, good selectivity, mild working temperature, and fast response of the polymer/nanoparticle hybrid films. We examine two copolymers, poly(3,4-ethylenedioxythiophene-*co*-thiophene-3-acetic acid)-(poly(EDOT-*co*-TAA)) and poly(3,4-ethylenedioxythiophene-*co*-thiophene-3-ethanol) (poly(EDOT-*co*-3-TE)), in order to compare the role of linker molecules and to determine the functional sensing mechanism.[12] The simple operation of the sensor and its direct applicability to PCBs illustrates potential of this technology in distributed low-cost wireless sensing of VOCs (Figure 2a).

2. EXPERIMENTAL PROCEDURE

Copolymer deposition. The oCVD technique has been described in many previous publications, and the structure of an oCVD reactor was reported by Bhattacharyya et al.[13] Poly(EDOT-*co*-3-TE) and poly(EDOT-*co*-TAA) were deposited at the stage temperature of 100 °C. 3,4-ethylenedioxythiophene (EDOT, CAS 126213-50-1, Sigma-Aldrich) was vaporized in a monomer jar at 140 °C. Thiophene-3-ethanol (3-TE, CAS 13781-67-4, Sigma-Aldrich) was vaporized at the temperature of 160−200 °C and thiophene-3-acetic acid (TAA, CAS 6964-21-2, Sigma-Aldrich) at a temperature of 200 °C. The monomers

DOI: 10.1021/acsami.5b05392
ACS Appl. Mater. Interfaces 2015, 7, 16213−16222

were introduced separately into the vacuum chamber. The relative amount of EDOT and 3-TE was controlled by varying the temperature of the monomer jar containing 3-TE. The valve opening extent for EDOT and 3-TE were kept the same, and the temperature of 3-TE varied from 160 to 180 to 200 °C. Contact angle results showed the composition change with different 3-TE monomer jar temperatures. The sensors whose sensing behavior was investigated were made with 200 °C 3-TE.The relative amount of EDOT and TAA was controlled by varying the extent of valve opening on the monomer lines. We kept the temperature of EDOT and TAA at 140 and 200 °C, respectively, and changed the extent of opening of EDOT and TAA from 1:1, 3:5 to 1:2. In sensor fabrication, we used 1:2 (EDOT:TAA) samples. $FeCl_3$ (CAS 7705-08-0, Sigma-Aldrich) was used as the oxidant at the temperature of 350 °C. The two kinds of copolymers were deposited on silicon wafers, glass slides, and printed circuit boards (PCBs).

The design of the resistive sensing elements on the PCB is shown in Figure 2b. Gray parts are electrodes and conducting wires. The copolymer films were deposited between the electrodes using a shadow mask. The picture of the device is shown in Figure S1. The resistance was measured between I1 and I2 in Figure 2b. The sheet resistances of the films were measured with 4-point probing system Jandel Model RM3. The thickness of film was measured by Veeco DEKTAK 150 profilometer.

Attachment of Gold Nanoparticles. The second step of the experiment was to attach gold nanoparticles covalently on the polymer films. The 6−21 mg 250 nm/50 nm diameter gold nanoparticles, purchased from Sigma-Aldrich, were treated with 20 mL of 0.1 M linker molecule solution in methanol at 80 °C for 2 h. In case of poly(EDOT-*co*-3-TE), the linker molecule used was methyl4-mercaptobenzoate (CAS 6302-65-4 purchased at Santa Cruz Biotechnology Inc.) or 4-mercaptobenzoic acid (CAS 1074-36-8 purchased from Sigma-Aldrich) and for poly(EDOT-*co*-TAA) the linker molecule was 4-aminothiophenol (CAS 1193-02-8 purchased from Sigma-Aldrich). After the treatment, the thiol reacted with Au particles and formed the Au−S−R bond. Then, 20 mL of 0.01 M N,N′-dicyclohexylcarbodiimide (DCC, CAS 538-75-0, purchased from Sigma-Aldrich) solution in methanol and 5 mL of 0.1 M 4-dimethylaminopyridine (DMAP, CAS 1122-58-3, purchased from Sigma-Aldrich) solution in methanol were prepared. The copolymer films (~5 cm^2) were treated by the mixture of the above solutions at 50 °C for 24 h. The sample surface was rinsed with fresh methanol for 5 min in order to remove residual DCC and DMAP. To investigate the mechanism, we also fabricated Ni nanoparticle−copolymer sensor and Pd nanoparticle−copolymer sensor on PCBs using the similar method in literature.[9]

Material characterization. The obtained copolymer films and copolymer-gold nanoparticle hybrid films were characterized by Fourier transform infrared spectroscopy (FTIR, Thermo Scientific Nicolet iS50 spectrometer), X-ray photoelectron spectroscopy (XPS, Surface Science Instruments SSX-100), contact angle (Rame-hart Inc. model 200−00), scanning electron microscope (SEM, JEOL 6010LA), energy-dispersive X-ray spectroscopy (EDS, JEOL 6010LA), and ultraviolet−visible absorption spectroscopy (UV−vis, Varian Inc. Cary 6000i).

Sensor test. The test of the sensing performance was conducted in a custom-made chamber (the system can be seen in Figure S2). The sensing elements were placed inside the test cell. Mass flow controllers (MFC) (MKS Instruments, Inc. Mass flow controller model 1479A and model M100B) and bubblers were used to flow nitrogen and analytes into the test cell. The bubblers were used to introduce the vapor of the liquid solvents such as methanol, water, acetone, and toluene. First, the test cell was purged with ~3200 sccm nitrogen. The analyte vapor was then introduced by flowing nitrogen through the bubbler at a flow rate of 10−50 sccm with an MFC, while keeping the purging nitrogen flow. This procedure gave a mixture of nitrogen and analyte vapor at low concentrations. Then the flow rate of analyte vapor is turned back to zero. We used the pure nitrogen to flush the test cell again. In the test of *n*-pentane response, a premixture of 7000 ppm *n*-pentane in nitrogen (purchased from Airgas) was used. Therefore, two MFCs were used to control the flow rate of nitrogen and the premixture. The flow rate of nitrogen was varied from 0 to 50 sccm and the flow rate of premixture from 50 to 0 sccm, with the total flow rate of 50 sccm. The corresponding resistance change was measured by Keithley 2400 SourceMeter and recorded on a computer. For films deposited on silicon wafer, two alligator clips were used as the electrical contacts to the conducting wires, whereas for PCB, metal contact pads were connected to the soldered pins. The temperature of the test cell was kept at 30 °C by an incubator and a water bath with a circulator (JEIO Tech IB-05G and NESLAB RTE-111). The volumetric concentration of the analyte in the gas mixture was estimated by the analyte's vapor pressure and the flow rates of analytes and nitrogen. Finally, gas chromatography (Agilent Technologies7890A) was used to verify the concentration of the analytes.

3. RESULTS AND DISCUSSION

We synthesized two different conducting copolymers, poly(EDOT-*co*-TAA) and poly(EDOT-*co*-3-TE) and tethered the gold nanoparticles to both using wet chemical processing. The chemical structure of the complexes is shown in Figure 3. The

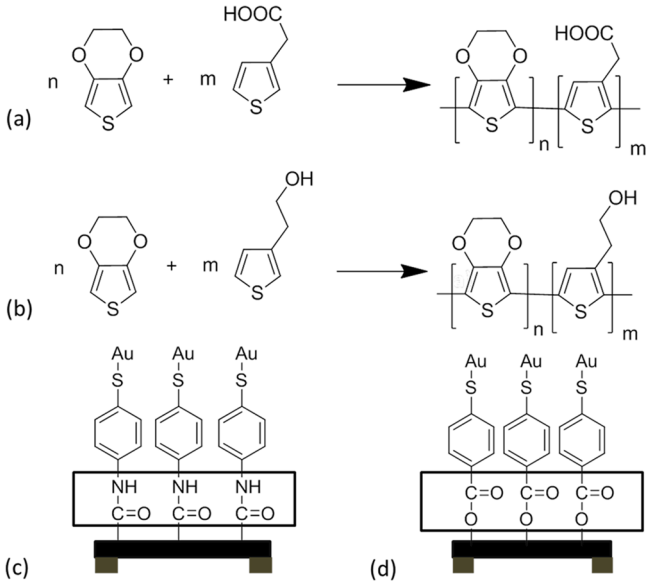

Figure 3. Chemical structure of the random copolymer films and the hybrid films. (a) The chemical structure of poly(EDOT-*co*-TAA), note the −COOH group introduced by TAA monomer. (b) The chemical structure of poly(EDOT-*co*-3-TE), note the −OH group introduced by 3-TE.[15] (c) poly(EDOT-*co*-TAA)/Au, showing the amide bonds formed between the polymer film and linker molecules. (d) poly(EDOT-*co*-3-TE), showing the ester bonds formed between the polymer film and linker molecules.

−COOH group in poly(EDOT-*co*-TAA) and the −OH group in poly(EDOT-*co*-3-TE) are the key terminal groups to form covalent bonds with the linker molecules and thus with the gold nanoparticles. The Fourier transform infrared (FTIR) spectrum of these oCVD polymers can be found in Figure S3. The peak of −OH (3427 cm^{-1}) is found in both poly(EDOT-*co*-TAA) and poly(EDOT-*co*-3-TE) as they both have the functional group in the film. The −C═O band at ~1600 cm^{-1} is found in poly(EDOT-*co*-TAA) as well, while this band is not found in PEDOT.

After the attachment of gold nanoparticles, the −C═O band can be found in poly(EDOT-*co*-3-TE)/Au film, which indicates the existence of the ester bond formed between the copolymer of poly(EDOT-*co*-3-TE) and the functionalized gold nanoparticles. In addition, −OH group is observed even after the

DOI: 10.1021/acsami.5b05392
ACS Appl. Mater. Interfaces 2015, 7, 16213−16222

Table 1. XPS Results

			poly(EDOT-*co*-TAA)		poly(EDOT-*co*-TAA)/Au		poly(EDOT-*co*-3-TE)		poly(EDOT-*co*-3-TE)/Au	
	peak	literature value(eV)	position (eV)	fwhm[a] (eV)	position (eV)	fwhm[a] (eV)	position (eV)	fwhm[a] (eV)	position (eV)	fwhm[a] (eV)
C 1s[16]	C−C and C−H	284.6	284.55	0.997	284.77	0.88	284.49	0.77	284.64	0.82
	C−S	285.2	285.65	1.16	285.67	1.09	285.25	0.95	285.39	0.97
	C−O	286.3	286.69	1.21	286.91	1.22	286.46	1.59	286.57	1.4
	COOH	288.8	288.48	1.46						
	N−C═O	289.8			289.21	1.38				
	COOR	∼289							289	1
N 1s[16]	N−H	399.7	none		399.56	1.22	none		not measurable	
	N−C═O	400.4			400.57	1.32				
Au 4f 7/2[17]	Au	83.86	none		83.86	1	none		83.85	0.83
	Au−S	84.57			84.27	1			84.57	1
Au 4f 5/2[17]	Au	87.58			87.75	0.69			87.55	1.07
	Au−S	89.12			88.56	1.53			89.12	1.9

[a]fwhm: Full Width at Half Maximum.

attachment of gold nanoparticles, which indicates that the −OH is not totally consumed by the Au-thiol component.

The X-ray photoelectron spectroscopy (XPS) results also supports the formation of covalent bonds in both poly(EDOT-*co*-TAA)/Au and poly(EDOT-*co*-3-TE)/Au films (Table 1). The detailed figures can be found in Figure S4. In accordance with Bhattacharyya et al.,[16] the XPS scans and the high resolution spectra of C 1s, N 1s, and Au 4f reveal the covalent bonding to the Au nanoparticles for both of the copolymers. The four samples used are poly(EDOT-*co*-TAA) film, the hybrid film of poly(EDOT-*co*-TAA)/Au, poly(EDOT-*co*-3-TE) film, and hybrid film of poly(EDOT-*co*-3-TE)/Au. In the C 1s spectra of all four samples, the EDOT comonomer units give rise to peaks corresponding to C−C and C−H (284.6 eV); C−S(285.2 eV); and C−O (286.3 eV). Additionally, the 3-TE and TAA comonomers also contribute to the intensity of these three peaks. The C 1s peak of −COOH (288.48 eV) is observed in poly(EDOT-*co*-TAA) film, confirming a successful copolymerization of EDOT and TAA. This peak shifts to 289.21 eV in poly(EDOT-*co*-TAA)/Au film as a consequence of amide bond formation (−N−C═O).[16]

The amide bond confirms the connection of gold nanoparticles to the film using a linker molecule. The amide bond provides a good electron path way[18] for transducing the resistance signal. N 1s spectra of poly(EDOT-*co*-TAA)/Au also reveal the amide bond in the hybrid film. As shown in Figure 4a, the −NH peak from the unreacted linker molecules is at 399.56 eV. The −N−C═O peak at 400.57 eV in the N 1s spectra provides evidence of amide bond forming. Note that no resolvable peaks are detected in the other three samples. In the high resolution spectra of Au 4f, the gold peaks are observed in both hybrid films (poly(EDOT-*co*-TAA)/Au and poly(EDOT-*co*-3-TE)/Au) as a result of gold immobilization. The Au 4f 7/2 peak ∼83.86 eV indicates the gold atom without bonding to any atoms.[17] The Au 4f 7/2 peak ∼84.57 eV indicates gold atom covalently linked to sulfur atom (Au−S), providing further evidence of bonding between the linker molecule and the gold nanoparticles.[17] The Au 4f 5/2 peaks of Au (87.58 eV) and Au−S (89.12 eV) also support the covalent linking of gold with linker molecules.[17] With all the evidence provided by XPS, the covalent bonding between the gold nanoparticles and the linker molecules as well as the linker molecules and the copolymer films are proved.

The synthesized copolymers are also characterized by contact angle. While the homopolymer of PEDOT has a contact angle of 84°,[19] copolymerization of EDOT with a more hydrophilic monomer causes both copolymers to have more hydrophilic surfaces than PEDOT. The contact angles and conductivities are shown in Table 2. Additionally, the conductivity of the copolymers is lower than that of PEDOT due to the incorporation of the comonomers 3-TE and TAA.

The scanning electron microscope (SEM) image verifies the presence of gold nanoparticles at the surface of the hybrid films. Figure 4b shows the surface of poly(EDOT-*co*-TAA) with 250 nm Au nanoparticles. The nanoparticles are attached on top of the copolymer films successfully. The SEM images of the hybrid films of poly(EDOT-*co*-3-TE)/Au can be found in Figure S5. Two different nanoparticle sizes, 250 and 50 nm, are investigated. The SEM images of 50 nm Au nanoparticle-poly(EDOT-*co*-TAA) samples and 250 nm Au nanoparticle-poly(EDOT-*co*-TAA) samples can be found in Figure S6. 50 nm Au nanoparticles tend to aggregate together as shown in the SEM image, compared to the 250 nm Au nanoparticles. This aggregation phenomenon may be due to the larger surface energy induced by smaller dimension.

Energy-dispersive X-ray spectroscopy (EDS) provides evidence for both the elementary composition of the particles shown in the SEM figures and the covalent bonding of gold nanoparticles and sulfur atoms. EDS images can be found in the Figure S7. Distribution of gold verifies that the nanoparticles shown in the original SEM images are Au. Additionally, the density of sulfur is consistent with the density distribution of gold, which implies the affinity of gold and sulfur and thus the covalent bonding of a nanoparticle with the sulfur atom in the linker molecule. Other element distributions do not show any significant pattern.

The UV−vis spectroscopy analysis confirms the existence of 250 nm diameter gold nanoparticle layers on the film. Figure 4c shows the UV−vis spectra of the poly(EDOT-*co*-TAA) film, Au-nanoparticle colloid, and the polymer−nanoparticle hybrid film. The peak centered at the 570 nm wavelength arises from the surface plasmon resonance of gold nanoparticles attached to the film.[20]

Following the chemical and material characterization, we investigate the resistive response of the device to methanol vapors. We define the resistive response as

DOI: 10.1021/acsami.5b05392
ACS Appl. Mater. Interfaces 2015, 7, 16213−16222

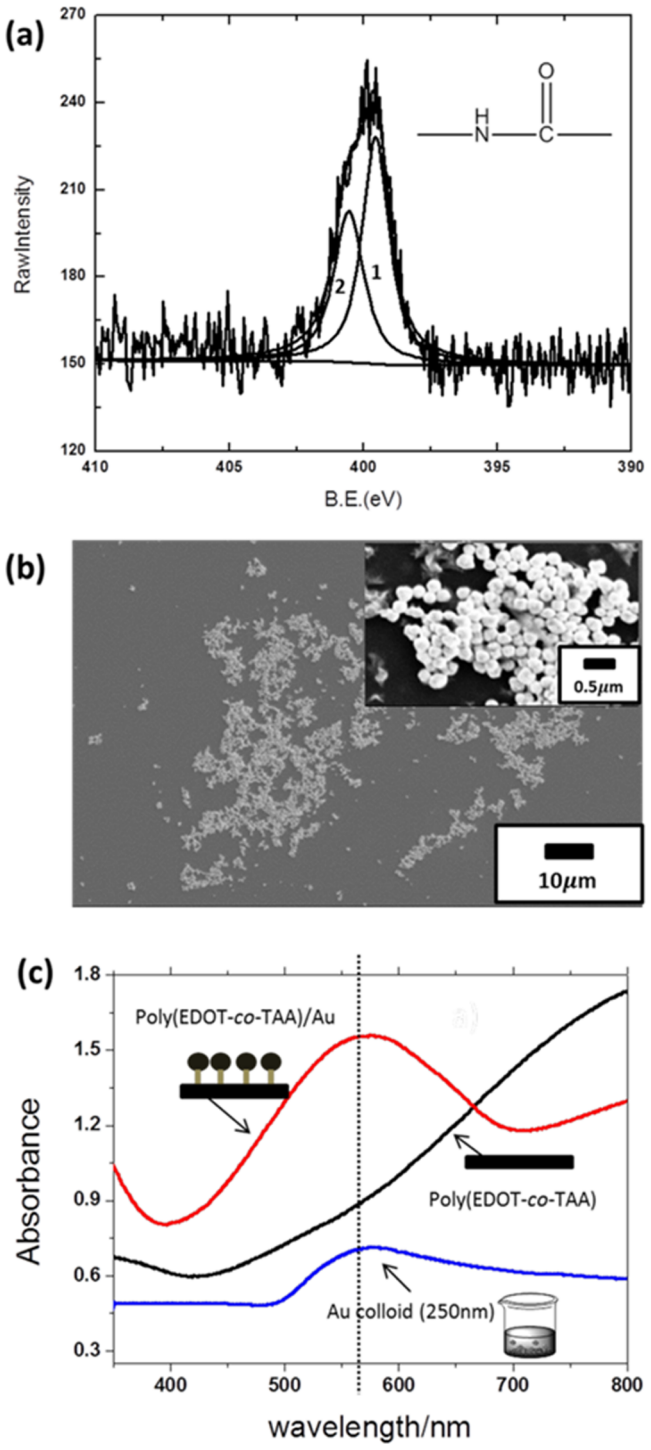

Figure 4. (a) XPS N 1s of poly(EDOT-*co*-TAA) /Au hybrid film, 1 is −NH, 2 is −N−C═O. (b) SEM image of the surface of hybrid film of poly(EDOT-*co*-TAA), showing 250 nm diameter nanoparticles with an inset showing a higher magnitude image of the same film, showing the dispersion of gold nanoparticles on the surface; (c) UV−vis spectra of the Au colloid (250 nm diameter) and the film with and without gold nanoparticles. A peak in the 570 nm wavelength region confirms the existence of gold nanoparticles.

$$\text{response} = \frac{R - R_0}{R_0} \times 100\% \quad (1)$$

where R_0 is the average value of the film resistance before introducing any analyte, and R is the resistance of the film. The response time is defined as the time needed to reach the 90% of the final response. The response of poly(EDOT-*co*-TAA)/Au (250 nm diameter) film deposited on Si wafer is shown in Figure 5a. The response to methanol is strong, and its magnitude was proportional to the concentration of the analyte.

Table 2. Advancing Contact Angles and the Conductivities for the Conducting Co-Polymer Films Synthesized at Substrate Temperature in Parentheses

sample name	contact angle (deg)	conductivity (S/cm)
PEDOT	81.5	352
poly(EDOT-*co*-3-TE)(160 °C)	54.8	90.1
poly(EDOT-*co*-3-TE)(180 °C)	37.9	15.3
poly(EDOT-*co*-3-TE)(200 °C)	32.3	3.24
poly(EDOT-*co*-TAA)(200 °C)	51.5	65.9

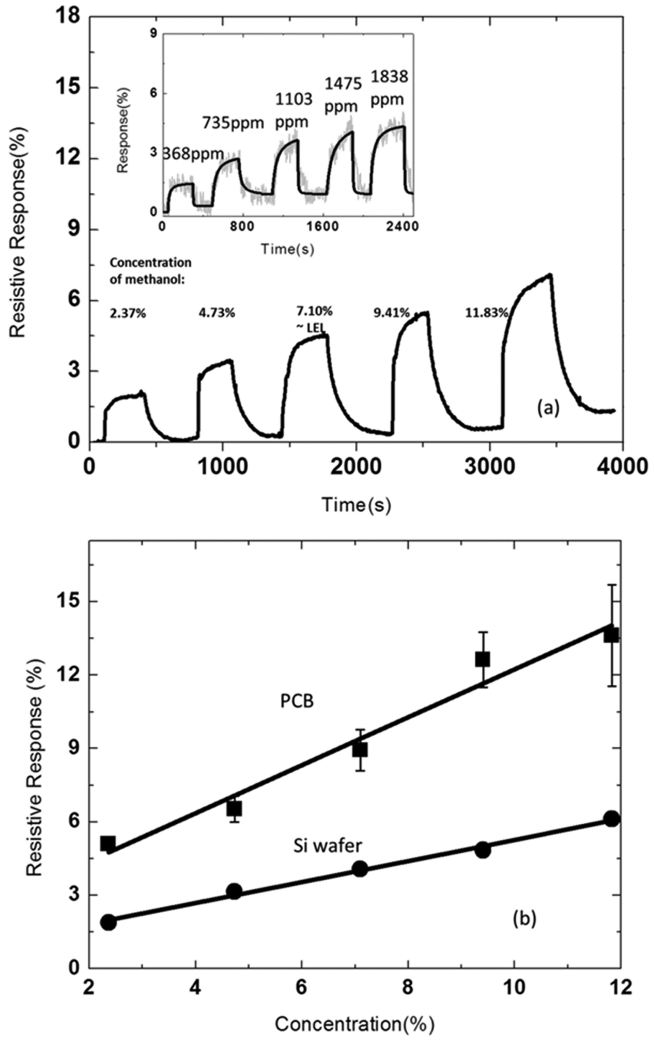

Figure 5. (a) Response of hybrid poly(EDOT-*co*-TAA) film with Au NPs (250 nm) deposited on Si wafer to methanol vapor. The inset is the response of the hybrid poly(EDOT-*co*-TAA) film with Au NPs (250 nm) deposited on PCB to lower concentrations of methanol. The signal was processed using a filter by assuming the signal obeys a saturating function. (b) Comparison of the response of hybrid poly(EDOT-*co*-TAA) film with Au NPs (250 nm) on PCB with the response of the hybrid film on Si wafer.

DOI: 10.1021/acsami.5b05392
ACS Appl. Mater. Interfaces 2015, 7, 16213−16222

Table 3. Summary of the Response of Four Different Samples

sample composition	gold nanoparticle diameter(nm)	substrate	response to MeOH (23665 ppm) (%)	response to MeOH (368 ppm) (%)	response time (T_{90}) (s)	recovery time (s)	projected detection limit (ppm) (at S/N = 3)
poly(EDOT-*co*-TAA)/Au hybrid film	250	Si wafer	1.89 ± 0.10	none	130−200	270−380	475
	50		2.30 ± 0.09	none	60−70	500−550	none
	250	PCB	5.09 ± 0.26	1.70 ± 0.36	120−220	130−200	171 (lowest concentration tested)
poly(EDOT-*co*-3-TE)/Au hybrid film	250		noisy, similar to polymer film response	none	>300	none	none

The response time was ∼100 s, sufficiently short for use in commercial sensing.

The response is improved by depositing the hybrid film on PCBs. As a result of better electrode contacts, the PCB sensor provides much larger response signal as shown in Figure 5b. The raw data of the sensing test are in Figure S8.

The inset in Figure 5a shows the response of poly(TAA-*co*-EDOT)/Au film on PCB at low concentrations. The short response time (∼200 s) is similarly to other samples based on hybrid poly(TAA-*co*-EDOT)/Au films. The signal also decreases proportionally with decreasing analyte concentration. The recovery time is comparable to the response time (∼200 s). In addition, the response is nearly reversible with >84% (the second peak) return to the baseline resistivity after each pulse.

The sensing characteristics of all the samples are summarized in Table 3. The raw data of the sensing tests can be found in Figure S8. We compare three factors that may influence the sensing behavior, the diameter of gold nanoparticles, the device contact type (films on silicon with alligators or films on PCBs), and the linker molecule. The responses of 50 nm Au nanoparticle samples do not increase with concentration increasing (Figure S8a). This phenomenon may be induced by the severe aggregation of the 50 nm gold nanoparticles limiting the available surface area. As shown in Table 3, the PCB enhanced the resistive response because of a better electrical contact. In addition, the linker molecule is of great importance in gas sensing. Although the poly(EDOT-*co*-TAA)/Au samples have a fast and reversible response to methanol, the poly(EDOT-*co*-3-TE)/Au samples do not exhibit meaningful response to methanol. We speculate that unlike the former type of samples, which have an amide bond between the copolymer and the linker molecule, the linker molecule used in the latter type of samples formed an ester bond instead, resulting in a significantly poorer response. The amide bond provides a good electron pathway because the N−C bond is a partial double bond and the four atoms, H, N, C, and O, are on the same plane.[18,21,22] This observation indicates that the sensing mechanism relies on the analyte influencing the work function of the metal nanoparticles and thus changing the electric resistance of the conducting polymer as discussed by previous researchers.[8,9] The sensor is also noticeably different from the monolayer Au nanoparticle sensor, since the film of poly-(EDOT-*co*-3-TE)/Au does not show a good response to methanol, even though the gold nanoparticles here are also functionalized with thiol. The only difference between poly(EDOT-*co*-3-TE)/Au and poly(EDOT-*co*-TAA)/Au films is different linking between gold nanoparticles and the polymer film. If a monolayer of gold nanoparticles is the reason for sensing behavior, the poly(EDOT-*co*-3-TE)/Au film should also respond to methanol, and moreover, similarly to the Au-monolayer sensor. This therefore suggests that it is not the monolayer of gold nanoparticles but the link between the metal nanoparticles and the polymer film that plays the key role in the sensing mechanism.

The response of the poly(EDOT-*co*-TAA)/Au hybrid films to different methanol concentrations is shown in Figure 6. We find that the overall resistive response of the device can be described with the Brunauer−Emmett−Teller (BET) theory of multilayer adsorption,[23] with a steep slope in initial concentrations shown in Figure 6a. The BET theory states

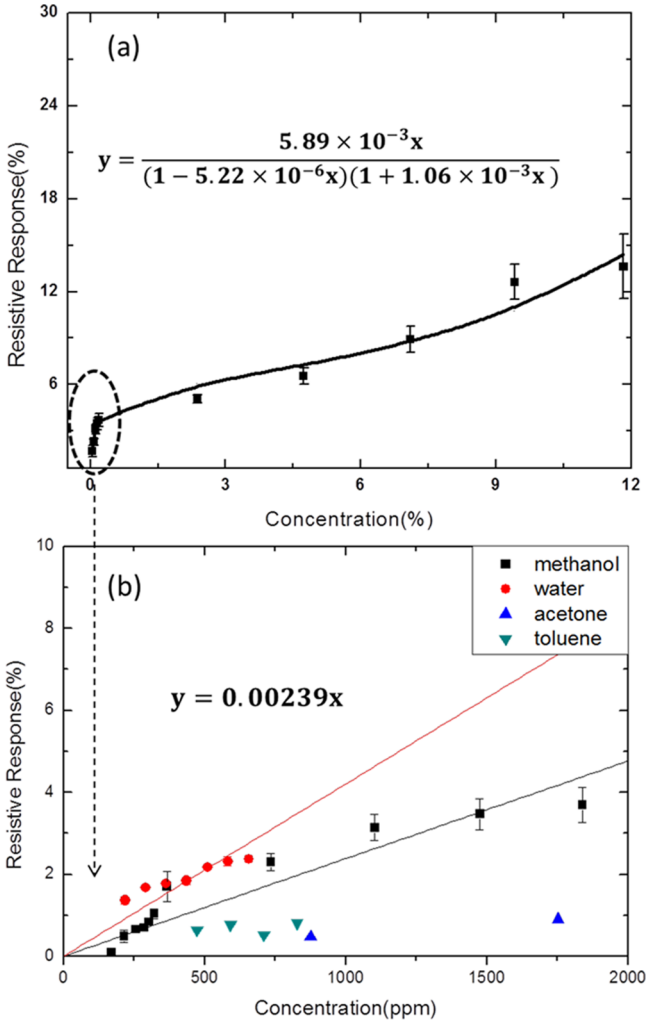

Figure 6. (a) Data points of response of poly(TAA-*co*-EDOT)/Au film on PCBs (points with error bars), and the fitting curve using BET adsorption equation (the solid line); (b) response of poly(TAA-*co*-EDOT)/Au film on PCBs to methanol vapor at low concentrations, together with the responses to water, acetone, and toluene vapors.

DOI: 10.1021/acsami.5b05392
ACS Appl. Mater. Interfaces 2015, 7, 16213−16222

$$V = \frac{\frac{YV_{max}p}{p_v}}{\left(1 - \frac{p}{p_v}\right)\left(1 + \frac{(Y-1)p}{p_v}\right)} \quad (2)$$

where V is the adsorbed gas volume, V_{max} denotes the volume needed to form a monolayer on the whole surface, p_v denotes the vapor pressure of the adsorbed gas, Y is a constant number, and $Y \approx \exp[((\Delta H_{des} - \Delta H_{vap})/(RT))]$, where ΔH_{des} is the heat of desorption, ΔH_{vap} is the heat of vaporization, R is the ideal gas constant, and T is the temperature.[23,24]

In the experiments analyzed here, the temperature was maintained at 30 °C, thus p_v is 21914 Pa. Under ideal gas assumption, $p = 0.101325x$ Pa and $(p/p_v) = 4.624 \times 10^{-6}x$, where x is the concentration in ppm. To take nonideality into consideration, we used a coefficient c so that $(p/p_v) = 4.624 \times 10^{-6}cx$. If we assume the response is proportional to the adsorbed gas volume, the BET equation to describe the relationship of response and methanol concentration is

$$\text{response} = \frac{4.624 \times 10^{-6}acx}{(1 - 4.624 \times 10^{-6}cx)(1 + 4.624 \times 10^{-6}bcx)} \quad (3)$$

Response is in percentage, x is in ppm, a and b are constant numbers related to the material. As shown in Figure 6a, in eq 3, a is 1129(%), b is 203.3, c is 1.128, and the coefficient of determination $R^2 = 0.97$. These parameters are determined by MATLAB nonlinear least-squares regression. The response of this device is in accordance with the indicating BET theory. In eq 3, a is proportional to YV_{max} and $b = Y - 1$ in eq 2. With $Y \approx \exp[((\Delta H_{des} - \Delta H_{vap})/(RT))]$ and ΔH_{vap} of methanol is 37.9 kJ/mol,[23] we calculate the heat of desorption as ΔH_{des} = 51.3 /mol. This value lies in the range of physisorption enthalpies (20−80 kJ/mol) for small molecules that interact with surfaces through van der Waals forces.[25] Figure 6b is the linear fitting of the response at low concentration regime. The lowest concentration tested is 171 ppm, with a response of ∼0.1%. This concentration is significantly less than 10% of the lower explosive limit (LEL) of methanol (6−6.7% by volume of air[26]). This detection limit is sufficient for sensors applied in refineries.[27] The response of the Au nanoparticle−copolymer sensor to water, acetone and toluene vapors are also investigated.

To investigate the sensing mechanism, we tested the sensor responses to water, acetone, and toluene. As shown in Figure 6b, the sensor responds to water vapor with high resistive response, whereas it shows poor sensitivity to toluene and acetone. The response to toluene does not increase with toluene concentration increasing. The change in the resistance may be due to film swelling afer toluene exposure. And the sensor does not respond to acetone vapor lower than 876 ppm. This phenomenon, together with the previous comparison between different linker molecules, leads us to propose a mechanism based on the hydrogen bonding among the analyte molecules and the work function change of the gold nanoparticles. We propose that molecules such as methanol and water first adsorb on the surface of gold nanoparticles. Because of hydrogen bonding among the analyte molecules, the negatively charged oxygen atom may interact with the slightly positively charged gold atom (not oxidized). In this way, the Fermi level of the gold nanoparticles will be increased, therefore the work function is changed accordingly. As Vaddiraju et al.[9] proposed, the potential barrier between the metal nanoparticle and the p-doped[9,28] semiconducting polymer poly(EDOT-*co*-TAA) is increased in this way, therefore the overall resistance increased. Although gold is usually considered noble, the weak interaction of oxygen atom and Au, and the electrostatic interaction between analytes and gold nanoparticles were reported by many researchers.[29−33] This weak interaction may have significant influence in the rest potential of Au.[29]

The Au nanoparticles may be slightly positively charged because they are covalently connected to the sulfur atom in the linker molecules. A priliminary calculation of Mulliken atomic charges supporting this assumption is included in Figure S9. In addition, the adsorbed molecule may also form hydrogen bonds with the amine group in the residual linker molecule ligands,[34,35] enhancing the Fermi level change of gold nanoparticles by moving the equilibrium. Another possible interaction is that the hydrogen bonding between the analyte molecules and the amide bond formed between the linker molecule and the copolymer film.[36,37]

Poly(TAA-*co*-EDOT)/Ni film and poly(TAA-*co*-EDOT)/Pd film on PCBs can also detect methanol vapor. The response of those sensors to methanol is shown in Figure S10. Oxygen atom interactions with palladium and nickel were reported before.[9] Similar hydrogen-bonding interactions with residual ligands also present here. It was also reported that Ni sensors had strong response to toluene and Pd sensors had strong response to acetone.[9] With these phenomena, sensor comprising Au, Ni, and Pd nanoparticles may respond to methanol, acetone, and toluene with different patterns, paving the way to a room temperature electro-nose.[38]

Assuming the resistive response of the sensor obeys BET theory leads to the hypothesis that the resistive response is linearly proportional to the adsorbed amount. In the Supporting Information, we include a simplified model based on the change of the work function in a Schottky diode. This model explains why the adsorbed amount and the resistive response have a proportional relationship.

Finally, the response of the bare copolymer films to methanol has been tested as well as sensing response of the poly(TAA-*co*-EDOT) film to other analytes. The results are shown in Figure S11. The response of the bare copolymer treated with the linker molecule to methanol is shown in Figure S12. For bare copolymers, the resistance of the film increases only marginally after exposure to methanol vapors, which may be due to the swelling of the film after adsorption of the methanol. Bare linker-molecule-treated copolymer shows little response to methanol vapor, which indicates that the interaction between the amide bond and the analytes may not dominate in the resistive response, given that amide bonds are also formed between the polymer film and the linker molecule in this case. For selectivity measurements, we choose acetone (876 ppm), toluene (710 ppm), and *n*-pentane (7000 ppm). With 876 ppm methanol, the interpolated response is 2.09%, while the measured response to 876 ppm acetone is 0.482%. With 710 ppm methanol, the interpolated response is 1.69%, whereas the measured response to toluene is 0.528%. With 7000 ppm methanol, the interpolated response is 5.08%, whereas with 7000 ppm *n*-pentane, the response (hard to see, resistance changed by ∼ 0.7%.) is slow and noisy. We use the definition of selectivity suggested by Homer, Zhou, Jewell, and Ryan[39] and Chen and Tan.[40] The selectivity is defined as

DOI: 10.1021/acsami.5b05392
ACS Appl. Mater. Interfaces 2015, 7, 16213−16222

$$\text{selectivity} = \frac{X_{max} - X_{min}}{X_{max} + X_{min}} \quad (4)$$

where X_{max} denotes the response of the device to the analyte which it has the largest response and X_{min} denotes the response to the analyte with lowest response.[39] If the X_{max} is the response to methanol and X_{min} is the response to other analytes with the same concentration, then the selectivity of methanol is 0.625 to acetone, 0.524 to toluene, and 0.758 to *n*-pentane. They are typical values for a sensor with good selectivity (selectivity ~0.5−1).[39,40]

Compared to other types of sensors, such as metal oxide sensors and conducting polymer film sensors, the poly(EDOT-*co*-TAA)/Au sensor has many unique advantages. First, the poly(EDOT-*co*-TAA)/Au sensor operates under room temperature, and the highest temperature that the printed circuit boards(PCBs) were exposed to in the fabrication process is 100 °C. Because PCBs are not able to sustain high temperatures, and the ability to deposit sensor directly on PCBs contributes to integration of the sensor into a wireless sensor network, this mild fabrication and test condition paves the way for an industrial sensor for refineries. With high sensitivity, metal oxide sensors are widely used in gas detection. However, depending on the fabrication methods and implementation environment of these sensors, some of them require high operating temperature (200−400 °C[41−43,46]) and some of them require high fabrication temperature (~400 °C-1000 °C[42,44,45]). High operation temperature may limit its application in refineries, and high fabrication temperature may limit its integration in PCBs. Therefore, the Au nanoparticle−copolymer sensor has unique advantage in the moderate working and fabrication temperatures.

Second, the metal nanoparticle−copolymer sensors have advantage in responding time, selectivity and magnitude of response, compared to bare conducting polymer film sensors. Conducting polymers are widely used in chemiresistors to detect Lewis acids and bases.[47,48] But the interaction of neutral molecules, such as alcohols is much less pronounced.[47] Because the dominating mechanism in detecting alcohols is swelling,[49] the responding time for conducting polymer sensors (typically ~14 min[49]) is significantly longer than our polymer−metal hybrid sensor (~100s). In addition, due to the swelling mechanism, the selectivity among organic solvent vapors is not ideal. While in the platform of covalently attached metal nanoparticle sensor, researchers are able to choose various metal nanoparticles to sense certain kinds of analytes specifically.[8,9] Polypyrrole was reported to respond to saturated methanol vapors with ~15% resistance change, which is comparable to our results.[47] However, other polymer sensors do not show such high response. For example, poly(3,3″-dipentoxy-2,2′:5′,2″-terthiophene) sensors showed only 0.2% response to saturated ethanol vapor.[48] The magnitude of our sensor is among the best values for bare conducting polymer film sensors.

4. CONCLUSIONS

In conclusion, economically feasible chemiresistive sensors based on gold nanoparticle/polymer hybrid films have been fabricated and characterized. The hybrid films of poly(EDOT-*co*-3-TE)/Au and poly(EDOT-*co*-TAA)/Au were deposited on Si wafers and printed circuit boards. The conducting copolymer films were deposited via substrate-independent oCVD method and further functionalized with solution-based nanoparticles. The poly(EDOT-*co*-TAA)/Au sensor exhibited a large and fast response (~100−200s) to methanol, with detection limit as low as 171 ppm. In addition, the sensor showed good analyte selectivity, having minimal sensing response to acetone, toluene, and *n*-pentane vapor.

The devices deposited on PCBs had significantly better performance than those on Si, mainly due to improved contacts between the oCVD-deposited film and the prepatterned PCB electrodes. This demonstrates not only the compatibility of the fabrication method with nonstandard substrates but also its excellent suitability for the circuit platforms readily usable in distributed wireless networks for efficient sensing of VOCs in petroleum industries. Examining different linker molecules between the nanoparticles and the copolymer films, we showed that the sensing mechanism originates from the interaction between oxygen atoms and metal nanoparticles induced by hydrogen bonding among the adsorbed analyte molecules, changing the work function of metal nanoparticles, and thus changing the resistance of the covalently connected copolymer films. The amide bond linkage between gold nanoparticles and poly(EDOT-*co*-TAA) films was shown to provide better electron pathway and thus better sensing performance. Finally, different combinations of copolymers and nanoparticle allow this method to be applicable to detection of a variety of other analytes.

■ ASSOCIATED CONTENT

Ⓢ Supporting Information

Picture of the PCB with electrodes bridged with the conducting polymer films; The schematic representation of the test system; FTIR results showing the covalent bonding of gold nanoparticles; XPS images of the hybrid films; SEM/EDS images of the metal/polymer hybrid film; SEM images comparing different Au nanoparticle sizes; Response of poly(EDOT-*co*-TAA)/gold nanoparticle(diameter 50 nm) film, poly(EDOT-*co*-3-TE)/gold nanoparticle(diameter 250 nm) film, and poly(EDOT-*co*-TAA)/gold nanoparticle(diameter 250 nm) film on PCBs ; The preliminary Mulliken atomic charge calculation of the linker molecule; Response of Ni nanoparticle−copolymer sensor to methanol vapors and response of Pd nanoparticle−copolymer sensor to methanol vapors; Response of copolymer/Au nanoparticle film and bare copolymer film to methanol, and PCB device response to toluene and *n*-pentane; Response of poly(EDOT-*co*-TAA) treated with 4-aminothiophenol to 1838 ppm methanol vapor; The model to explain the linear relationship between the adsorption amount and the resistive response. The Supporting Information is available free of charge on the ACS Publications website at DOI: 10.1021/acsami.5b05392.

■ AUTHOR INFORMATION

Corresponding Author

*E-mail: kkg@mit.edu.

Author Contributions

The manuscript was written through contributions of all authors. All authors have given approval to the final version of the manuscript.

Funding

Shell Oil Co.

Notes

The authors declare no competing financial interest.

DOI: 10.1021/acsami.5b05392
ACS Appl. Mater. Interfaces 2015, 7, 16213−16222

■ ACKNOWLEDGMENTS

We thank Royal Dutch Shell plc. for providing funding to this project. H.G., on-leave from Physics Department of Canakkale Onsekiz Mart University, was supported by TUBITAK Turkey.

■ REFERENCES

(1) Pejcic, B.; Eadington, P.; Ross, A. Environmental Monitoring of Hydrocarbons: A Chemical Sensor Perspective. *Environ. Sci. Technol.* **2007**, *41* (18), 6333−6342.
(2) Savazzi, S.; Guardiano, S.; Spagnolini, U. Wireless Sensor Network Modeling and Deployment Challenges in Oil and Gas Refinery Plants. *Int. J. Distrib. Sens. Networks* **2013**, *2013*, No. 383168.
(3) Saha, K.; Agasti, S. S.; Kim, C.; Li, X.; Rotello, V. M. Gold Nanoparticles in Chemical and Biological Sensing. *Chem. Rev.* **2012**, *112* (5), 2739−2779.
(4) Grate, J. W.; Nelson, D. A.; Skaggs, R. Sorptive Behavior of Monolayer-Protected Gold Nanoparticle Films: Implications for Chemical Vapor Sensing. *Anal. Chem.* **2003**, *75* (8), 1868−1878.
(5) Ibanez, F. J.; Zamborini, F. P. Chemiresistive Sensing with Chemically Modified Metal and Alloy Nanoparticles. *Small* **2012**, *8* (2), 174−202.
(6) Zhang, H.; Evans, S. D.; Henderson, J. R.; Miles, R. E.; Shen, T. Vapor Sensing Using Surface Functionalized Gold Nanoparticles. *Nanotechnology* **2002**, *13* (3), 439−444.
(7) Kim, Y. J.; Yang, Y. S.; Ha, S. C.; Cho, S. M.; Kim, Y. S.; Kim, H. Y.; Yang, H.; Kim, Y. T. Mixed-Ligand Nanoparticles of Chlorobenzenemethanethiol and N-octanethiol as Chemical Sensors. *Sens. Actuators, B* **2005**, *106* (1), 189−198.
(8) Vaddiraju, S.; Seneca, K.; Gleason, K. K. Novel Strategies for the Deposition of -COOH Functionalized Conducting Copolymer Films and the Assembly of Inorganic Nanoparticles on Conducting Polymer Platforms. *Adv. Funct. Mater.* **2008**, *18* (13), 1929−1938.
(9) Vaddiraju, S.; Gleason, K. Selective Sensing of Volatile Organic Compounds Using Novel Conducting Polymer-Metal Nanoparticle Hybrids. *Nanotechnology* **2010**, *21* (12), 125503−125511.
(10) Laforgue, A.; Robitaille, L. Production of Conductive PEDOT Nanofibers by the Combination of Electrospinning and Vapor-Phase Polymerization. *Macromolecules* **2010**, *43* (9), 4194−4200.
(11) Kwon, O. S.; Park, S. J.; Lee, J. S.; Park, E.; Kim, T.; Park, H.-W.; You, S. A.; Yoon, H.; Jang, J. Multidimensional Conducting Polymer Nanotubes for Ultrasensitive Chemical Nerve Agent Sensing. *Nano Lett.* **2012**, *12* (6), 2797−2802.
(12) Fu, B.; Baltazar, J.; Sankar, A. R.; Chu, P. H.; Zhang, S.; Collard, D. M.; Reichmanis, E. Enhancing Field-Effect Mobility of Conjugated Polymers Through Rational Design of Branched Side Chains. *Adv. Funct. Mater.* **2014**, *24* (24), 3734−3744.
(13) Bhattacharyya, D.; Howden, R. M.; Borrelli, D. C.; Gleason, K. K. Vapor Phase Oxidative Synthesis of Conjugated Polymers and Applications. *J. Polym. Sci., Part B: Polym. Phys.* **2012**, *50* (19), 1329−1351.
(14) Bhattacharyya, D.; Kim, T.; Pal, S. A Comparative Study of Wireless Sensor Networks and Their Routing Protocols. *Sensors* **2010**, *10* (12), 10506−10523.
(15) Bhattacharyya, D.; Senecal, K.; Marek, P.; Senecal, A.; Gleason, K. K. High Surface Area Flexible Chemiresistive Biosensor by Oxidative Chemical Vapor Deposition. *Adv. Funct. Mater.* **2011**, *21* (22), 4328−4337.
(16) Bhattacharyya, D.; Gleason, K. K. Single-step Oxidative Chemical Vapor Deposition of -COOH Functional Conducting Copolymer and Immobilization of Biomolecule for Sensor Application. *Chem. Mater.* **2011**, *23* (10), 2600−2605.
(17) Vitale, R.; Fratoddi, I.; Battocchio, C.; Piscopiello, E.; Tapfer, L.; Russo, M. V.; Polzonetti, G.; Giannini, C. Mono- and Bi-Functional Arenethiols as Surfactants for Gold Nanoparticles: Synthesis and Characterization. *Nanoscale Res. Lett.* **2011**, *6*, 103.
(18) Sewald, N.; Jakubke, H. D. *Peptides: Chemistry and Biology*, 2nd ed.; Wiley−VCH: Weinheim, Germany, 2009.
(19) Im, S. G.; Kusters, D.; Choi, W.; Baxamusa, S. H.; van de Sanden, M. C. M.; Gleason, K. K. Conformal Coverage of Poly(3,4-ethylenedioxythiophene) Films with Tunable Nanoporosity via Oxidative Chemical Vapor Deposition. *ACS Nano* **2008**, *2* (9), 1959−1967.
(20) Haiss, W.; Thanh, N. T. K.; Aveyard, J.; Fernig, D. G. Determination of Size and Concentration of Gold Nanoparticles from UV-vis Spectra. *Anal. Chem.* **2007**, *79* (11), 4215−4221.
(21) Wang, Q.; Xia, X.; Huang, W.; Lin, Y.; Xu, Q.; Kaplan, D. L. High Throughput Screening of Dynamic Silk-Elastin-Like Protein Biomaterials. *Adv. Funct. Mater.* **2014**, *24* (27), 4303−4310.
(22) Huang, W.; Krishnaji, S.; Hu, X.; Kaplan, D.; Cebe, P. Heat Capacity of Spider Silk-Like Block Copolymers. *Macromolecules* **2011**, *44* (13), 5299−5309.
(23) Atkins, P.; Paula, J. d. *Physical Chemistry*, 8th ed.; Oxford University Press: New York, 2006.
(24) Lau, K. K. S.; Gleason, K. Initiated Chemical Vapor Deposition (iCVD) of Poly(alkyl acrylates): An Experimental Study. *Macromolecules* **2006**, *39* (10), 3688−3694.
(25) Hayward, D. O.; Trapnell, B. M. W. *Chemisorption*, 2nd ed.; Butterworths: London, 1964.
(26) Hamaker, K. H.; Johnson, D. C.; Bellucci, J. J.; Apgar, K. R.; Soslow, S.; Gercke, J. C.; Menzo, D. J.; Ton, C. Design of a Novel Automated Methanol Feed System for Pilot-Scale Fermentation of Pichia Pastoris. *Biotechnol. Prog.* **2011**, *27* (3), 657−667.
(27) Keller, C. L. Future Requirements for Unrestricted Entry into Confined Spaces. *Plant/Oper. Prog.* **1987**, *6* (3), 142−145.
(28) Im, S. G.; Gleason, K. K.; Olivetti, E. A. Doping Level and Work Function Control in Oxidative Chemical Vapor Deposited Poly(3,4-Ethylenedioxythiophene). *Appl. Phys. Lett.* **2007**, *90* (15), 152112.
(29) Hoare, J. P. A Study of the Rest Potentials in the Gold-Oxygen-Acid System. *J. Electrochem. Soc.* **1963**, *110* (4), 245−249.
(30) Phillips, R. L.; Miranda, O. R.; You, C.-C.; Rotello, V. M.; Bunz, U. H. F. Rapid and Efficient Identification of Bacteria Using Gold-Nanoparticle-Poly(para-phenyleneethynylene) Constructs. *Angew. Chem., Int. Ed.* **2008**, *47* (14), 2590−2594.
(31) Hoare, J. P. A Cyclic Voltammetric Study of the Gold-Oxygen System. *J. Electrochem. Soc.* **1984**, *131* (8), 1808−1815.
(32) Lopez, N.; Norskov, J. K. Catalytic CO Oxidation by a Gold Nanoparticle: A Density Functional Study. *J. Am. Chem. Soc.* **2002**, *124* (38), 11262−11263.
(33) Calzolai, L.; Franchini, F.; Gilliland, D.; Rossi, F. Protein-Nanoparticle Interaction: Identification of the Ubiquitin-Gold Nanoparticle Interaction Site. *Nano Lett.* **2010**, *10* (8), 3101−3105.
(34) Aubin-Tam, M.-E.; Hamad-Schifferli, K. Gold Nanoparticle-Cytochrome c Complexes: The effect of Nanoparticle Ligand Charge on Protein Structure. *Langmuir* **2005**, *21* (26), 12080−12084.
(35) Ai, K.; Liu, Y.; Lu, L. Hydrogen-Bonding Recognition-Induced Color Change of Gold Nanoparticles for Visual Detection of Melamine in Raw Milk and Infant Formula. *J. Am. Chem. Soc.* **2009**, *131* (27), 9496−9497.
(36) Cooper, E.; Leggett, G. J. Influence of Tail-Group Hydrogen Bonding on the Stailities of Self-Assembled Monolayers of Alkythiols on Gold. *Langmuir* **1998**, *15* (4), 1024−1032.
(37) Boal, A. K.; Rotello, V. M. Intra-and Intermonolayer Hydrogen Bonding in Amide-Functionalized Alkanethiol Self-Assembled Monolayers on Gold Nanoparticles. *Langmuir* **2000**, *16* (24), 9527−9532.
(38) Rock, F.; Barsan, N.; Weimar, U. Electronic Nose: Current Status and Future Trends. *Chem. Rev.* **2008**, *108* (2), 705−725.
(39) Homer, M. L.; Zhou, H.; Jewell, A. D.; Ryan, M. A. *Computational Methods for Sensor Material Selection*, 1st ed.; Springer: New York, 2010.
(40) Chen, Y.; Tan, T. C. Selectivity Enhancement of an Immobilized Apple Powder Enzymatic Sensor for Dopamine. *Biosens. Bioelectron.* **1993**, *9* (6), 401−410.
(41) Tomchenko, A. A.; Harmer, G. P.; Marquis, B. T.; Allen, J. W. Semiconducting Metal Oxide Sensor Array for the Selective Detection of Combustion Gases. *Sens. Actuators, B* **2003**, *93* (1), 126−134.

DOI: 10.1021/acsami.5b05392
ACS Appl. Mater. Interfaces 2015, 7, 16213−16222

(42) Mishra, V. N.; Agarwal, R. P. Sensitivity, Response and Recovery Time of SnO2 Based Thick-Film Sensor Array for H2, CO, CH4 and LPG. *Microelectron. J.* **1998**, *29* (11), 861−874.
(43) Kohl, D.; Heinert, L.; Bock, J.; Hofmann, T.; Schieberle, P. Systematic Studies on Response of Metal-Oxide Sensor Surfaces to Straight Chain Alkanes, Alcohols, Aldehydes, Ketones, Acids and Esters Using the SOMMSA Approach. *Sens. Actuators, B* **2000**, *70* (1), 43−50.
(44) Patel, N. G.; Patel, P. D.; Vaishnav, V. S. Indium Tin Oxide (ITO) Thin Film Gas Sensor for Detection of Methanol at Room Temperature. *Sens. Actuators, B* **2003**, *96* (1), 180−189.
(45) Kolmakov, A.; Klenov, D. O.; Lilach, Y.; Stemmer, S.; Moskovits, M. Enhanced Gas Sensing by Individual SnO2 Nanowires and Nanobelts Functionalized with Pd Catalyst Particles. *Nano Lett.* **2005**, *5* (4), 667−673.
(46) Baruwati, B.; Kumar, D. K.; Manorama, S. V. Hydrothermal Synthesis of Highly Crystalline ZnO Nanoparticles: A Competitive Sensor for LPG and EtOH. *Sens. Actuators, B* **2006**, *119* (2), 676−682.
(47) Charlesworth, J. M.; Partridge, A. C.; Garrard, N. Mechanistic Studies on the Interactions Between Poly(pyrrole) and Organic Vapors. *J. Phys. Chem.* **1993**, *97* (20), 5418−5423.
(48) Torsi, L.; Tanese, M. C.; Cioffi, N.; Gallazzi, M. C.; Sabbatini, L.; Zambonin, P. G.; Raos, G.; Meille, S. V.; Giangregorio, M. M. Side-Chain Role in Chemically Sensing Conducting Polymer Field-Effect Transistors. *J. Phys. Chem. B* **2003**, *107* (31), 7589−7594.
(49) Ak, M.; Yigitsoy, B.; Yagci, Y.; Toppare, L. Gas Sensing Property of a Conducting Copolymer. *e-Polym.* **2007**, *7* (1), 495−502.

DOI: 10.1021/acsami.5b05392
ACS Appl. Mater. Interfaces 2015, 7, 16213−16222